(2)

MTL TR 92-13

AD

STRUCTURAL TESTING EFFORTS FOR M-102 HOWITZER SUBLENGTH COMPOSITE CRADLE

PAUL V. CAVALLARO, DONALD W. OPLINGER,
KANU R. GANDHI, and GREGG J. PIPER
MECHANICS AND STRUCTURES BRANCH

ROBERT PASTERNAK
MATERIALS TESTING AND EVALUATION BRANCH

March 1992

Approved for public release; distribution unlimited.

US ARMY
LABORATORY COMMAND
MATERIALS TECHNOLOGY LABORATORY

U.S. ARMY MATERIALS TECHNOLOGY LABORATORY
Watertown, Massachusetts 02172-0001

The findings in this report are not to be construed as an official Department of the Army position, unless so designated by other authorized documents.

Mention of any trade names or manufacturers in this report shall not be construed as advertising nor as an official indorsement or approval of such products or companies by the United States Government.

DISPOSITION INSTRUCTIONS

Destroy this report when it is no longer needed.
Do not return it to the originator.

UNCLASSIFIED

SECURITY CLASSIFICATION OF THIS PAGE *(When Data Entered)*

REPORT DOCUMENTATION PAGE		READ INSTRUCTIONS BEFORE COMPLETING FORM
1. REPORT NUMBER MTL TR 92-13	2. GOVT ACCESSION NO.	3. RECIPIENT'S CATALOG NUMBER
4. TITLE *(and Subtitle)* STRUCTURAL TESTING EFFORTS FOR M-102 HOWITZER SUBLENGTH COMPOSITE CRADLE		5. TYPE OF REPORT & PERIOD COVERED Final Report 6. PERFORMING ORG. REPORT NUMBER
7. AUTHOR(s) Paul V. Cavallaro, Donald W. Oplinger,* Kanu R. Gandhi, Gregg J. Piper,† and Robert Pasternak		8. CONTRACT OR GRANT NUMBER(s)
9. PERFORMING ORGANIZATION NAME AND ADDRESS U.S. Army Materials Technology Laboratory Watertown, Massachusetts 02172-0001 SLCMT-MRS		10. PROGRAM ELEMENT, PROJECT, TASK AREA & WORK UNIT NUMBERS D/A Project: 1L162105.AH84
11. CONTROLLING OFFICE NAME AND ADDRESS U.S. Army Laboratory Command 2800 Powder Mill Road Adelphi, Maryland 20783-1145		12. REPORT DATE March 1992 13. NUMBER OF PAGES 30
14. MONITORING AGENCY NAME & ADDRESS *(if different from Controlling Office)*		15. SECURITY CLASS. *(of this report)* Unclassified 15a. DECLASSIFICATION/DOWNGRADING SCHEDULE

16. DISTRIBUTION STATEMENT *(of this Report)*

Approved for public release; distribution unlimited.

17. DISTRIBUTION STATEMENT *(of the abstract entered in Block 20, if different from Report)*

18. SUPPLEMENTARY NOTES

*Presently at Federal Aviation Administration Technology Center, Atlantic City International Airport, NJ 08405
†Presently at AMALGA Composites, Inc., 10600 W. Mitchell Street, West Allis, WI 53214

19. KEY WORDS *(Continue on reverse side if necessary and identify by block number)*

Howitzer (105 mm)	Graphite expoxy composite
Composites	Prototype testing
Fiber reinforced composites	Weight reduction
Structural integrity	Strength weight ratio

20. ABSTRACT *(Continue on reverse side if necessary and identify by block number)*

(SEE REVERSE SIDE)

DD FORM 1 JAN 73 1473 EDITION OF 1 NOV 65 IS OBSOLETE

UNCLASSIFIED

SECURITY CLASSIFICATION OF THIS PAGE *(When Data Entered)*

Block No. 20

ABSTRACT

In support of the U.S. Army's *Lightening the Force* effort, the U.S. Army Materials Technology Laboratory (MTL) is conducting prototype development of artillery system components. The use of advanced materials such as fiber reinforced composites provides the key to obtaining considerable weight reductions without compromising structural integrity. Composite materials offer significant strength-to-weight ratios as well as unique tailorability features to suit the needs of the design engineer. Currently, composite applications to the M-102, 105 mm Howitzer system are in progress. This report discusses the related testing activities used to evaluate the present composite cradle design.

CONTENTS

INTRODUCTION

The U.S. Army Materials Technology Laboratory's (MTL) major thrust in the M-102 Howitzer effort was to develop a composite technology demonstrator of the aluminum cradle, as shown in Figure 1a. A detailed discussion of the composite cradle design is given in References 1 and 2. The cradle serves to support and maintain alignment of the gun barrel during the recoil stroke, as well as provide a means of transferring the firing loads from the recoil mechanism to the trunnions. Firing loads are transmitted to the cradle through the recoil rod, as shown in Figure 1b. The recoil rod pulls against the front endplate which in turn distributes a compressive force over the cradle cross section. The cradle component was selected because it provided potential weight reductions through a redesign process utilizing state-of-the-art materials and engineering.

STRUCTURAL TESTING

Evaluation of the composite cradle design during the preliminary development stage was necessary to determine its structural behavior under simulated static, and dynamic loading conditions; more specifically, initial prototype tests were restricted to simulated recoil loads. Secondary loads and reactions were not to be included during the initial evaluation. The full scale prototype is shown in Figure 2 along with detailed section and component views. Manufacturing issues, however, dictated the use of sublength prototypes for the initial evaluation. Geometry of the first sublength cradle is shown in Figure 3. Longitudinal dimensions were reduced to roughly one-third of the full-scale cradle. Transverse or section dimensions remained true to scale. Possible effects associated with length reduction were investigated.

The first prototype was manufactured using both Fiberite HYE 1048AlC/104™ graphite/epoxy prepreg tape and Hercules AS-4™ graphite fiber. A Rohacell™ foam bulkhead was provided for buckling stability, as indicated in the section view A-A of Figure 2. Manufacturing processes for the various thin-walled components consisted of both hand layup (channels, V-wall, U-wall, and front and rear endplates) and filament winding techniques (tubes). Fiber orientations for the hand layup components were quasi-isotropic; i.e., 0°, 90°, and $\pm 45^{\circ}$. The filament winding pattern was $\pm 15^{\circ}$, $\pm 45^{\circ}$, $\pm 15^{\circ}$, 90°, and 90°. All components were adhesively bonded in the assembly stage using FM97 epoxy film adhesive produced by American Cyanamide™. The compressive modulus of the quasi-isotropic layup was obtained by using the ASTM D 3410-87 (Iitri specimen) test procedure. Several compressive stress-strain curves are shown in Figure 4. The average compressive modulus was 5.4×10^{6} psi. Although the specimens were not loaded to failure, the maximum induced compressive strain was 0.78% with only a slight deviation from linearity.

Live firing tests were performed on the existing M-102 Howitzer system at the U.S. Armament Research Development and Engineering Center (ARDEC) for two purposes:

1. GANDHI, K. R., CAVALLARO, P. V., and OPLINGER, D. W. Proceedings from Army Symposium on Solid Mechanics, Design, Analysis and Testing of Composite Components for the M-102 Howitzer, U.S. Army Materials Technology Laboratory, 1986.
2. OPLINGER, D. W., GANDHI, K. R., and CAVALLARO, P. V. Proceedings from Composite Materials in Armament Applications, v. I, AMMRC's Composite Howitzer Effort, U.S. Army Materials Technology Laboratory; also presented at Plastics Technology Evaluation Center, U.S. Armament Research Development and Engineering Center, 1985.

- To determine the maximum recoil rod pull force (P_r) sustained by the aluminum cradle. This force served as the primary loading mechanism in the design and test phases of the composite cradle.
- To compare the measured P_r with the analytically obtained value from the aluminum cradle stress analysis.[3] Using Zone VII ammunition (maximum charge) with the short recoil condition at a 70^o elevation angle, test results indicated the value of P_r was 24,000 lbs. The reported value of Reference 3 was 30% less than its measured counterpart. A summary of cradle loads and reactions from Reference 3 is shown in Figure 5.

The purpose of the sublength cradle testing effort was twofold. Experimental verification of the current prototype design was required to:

- Test the composite cradle to prescribed static and dynamic recoil loads obtained from field firing tests.
- Determine the internal strain distributions within the cradle components as an assembly.

Attachments such as elevation bracket/plug assemblies, trunnion plates, and bearing strips were not incorporated in the sublength evaluations. These components were to be evaluated individually and then incorporated into full-scale prototype cradle for further evaluation. A graphical description of the various loading configurations and brief result summary are presented in Figure 6 for each test.

Static Test #1

Static tests were aimed at applying a simulated recoil force of 45,000 lbs. (kips) to the cradle in the axial direction. (Later, during fatigue testing the maximum applied load was reduced to 24 kips in keeping with standard design philosophy which requires survival at limit load during cyclic loading.) This force was selected since it was the critical buckling load[1] of the aluminum cradle and it maintained a necessary margin of safety. The composite cradle design was found to be plate buckling sensitive along the free spans of the U-wall's bottom edge (refer to Figure 2) rather than Euler buckling of the entire cradle. These free spans behave as thin, narrow, and long strips under compressive loading with conservative, simply supported boundary conditions. As the length parameter increased beyond several widths, the effect of overall length ceased to influence the plate buckling load.[4] Furthermore, the presence of the foam bulkhead ensured a higher buckling mode; i.e., a full sine wave compared to a half sine wave along the transverse direction, thus raising the critical plate buckling load. Therefore, plate buckling loads for the full and sublength composite cradles were equivalent.

Loading was accomplished by compressing the cradle between the platens of a servo-hydraulic 60 kip tension/compression machine. For the initial test, the applied load was transferred from the upper machine platen to the cradle by way of a 1.25" diameter bolt positioned in the recoil rod hole of the graphite endplate. Loading through the bolt head simulated the presence of the actual recoil rod nut and pulling force, P_r, reacted by the cradle during firing. Instrumentation consisted of 16 uniaxial and two biaxial, 350 ohm strain gages

3. VEVLE, M.A. *Stress Analysis for the Howitzer, Light, Towed 105 mm: XM 102 Prototype II TN:9-63.* Rock Island Arsenal Research and Development Division, Design Engineering Branch, Rock Island, IL.
4. JONES, R. M. Mechanics of Composite Materials. Hemisphere Corporation, 1975.

bonded to the cradle with Eastman 910™ adhesive. Fifteen uniaxial gages were located in various regions where potentially high compressive and buckling strains were expected to exist. Two biaxial and one uniaxial gage were bonded to the top surface of the graphite endplate to measure bending strains. A strain gage location map is shown in Figure 7. All strains were monitored using the MEGADAC™ data acquisition system at thousand pound (1 kip) increments. Loading was stopped at 13.5 kips when the adhesive layer between the graphite endplate and the U-wall (outer skin) partially separated. It was this bond that secured the endplate to the cradle. The bond failed due to excessively high adhesive peel (transverse normal tensile) stresses which were inherent in the endplate design. As a result, no considerable amount of load was transferred from the endplate to the U-wall which then resulted in an overloaded condition on the V-wall (inner skin). The strain data supported this conclusion. The peak V-wall strain was measured at gage #7 with a value of 1804 microstrains (10^{-6} inches/inch) in compression. Strain at U-wall gage #18 was essentially zero. It should be noted that the in-plane stiffnesses of the U-wall and V-wall were equivalent since their thicknesses and fiber orientations were the same. Out-of-plane bending deformation of the graphite endplate was visually observed and existed due to inadequate flexural stiffness. Furthermore, lack of flexural stiffness resulted in debonding of the tensile side graphite bearing plate. At the 13.5 kip load level, the maximum endplate bending strain was 2460 microstrains in tension. This peak value occurred at the bottom edge of the endplate at gage #5. It should, however, be noted that the adhesive layer along this edge was maintained. Referring again to Figure 2, the foam bulkhead provided additional bonding area which locally enhanced the strength of the adhesive bond layer.

The behavior of the simplified beam/spring model of Figure 8 was synonymous with that of the endplate. Essentially, the endplate acted as a beam supported on four springs of equal stiffness. Since the flexural stiffness of the endplate (beam) was significantly less than the in-plane stiffness of the U-wall and V-wall (springs), it follows that the bending deflection at the center of the endplate was greater than the axial displacement of the cradle. This condition forced the outer edges of the endplate to pull away from the cradle and stress the adhesive layer in tension along the transverse normal direction.

Data inspection revealed a significant lack of correlation in strain readings between gages located symmetrically with respect to the cradle centerline. This lack of correlation was directly attributed to dimensional variations existing within the cradle. Inspection revealed, for example, that one side of the cradle was 0.062" longer than the other. These variations were a result of out-of-tolerance machining and possible component slippage during the assembly cure cycle. Thermoelastic expansion of the aluminum molds at recommended curing temperatures was subsequently discovered to have forced the thin walled components out-of-tolerance. Two additional cycles were performed to determine the repeatability of the previous strain readings.

Static Test #2

A second set of static tests was performed using a modified front endplate configuration. First, the graphite bearing plates were removed from the front endplate. An aluminum 6061-T6, 1" thick plate was then positioned on the top surface of the endplate to provide additional bending stiffness and to eliminate the previous endplate deflections. This modification was not intended to serve as a design solution but rather as a means of showing that a more uniform load distribution could be obtained with a stiffer endplate. Although the graphite endplate was not completely bonded to the cradle, its presence prevented the aluminum

plate from crushing (bearing failure) the ends of the thin walled components. A 2" diameter steel ball was placed in the recoil rod hole of the aluminum plate to reduce the effects of any loading eccentricities and to maintain an effective point load. The path of the applied load was then directed through the center of the ball. During the second test, the gages were monitored in a continuous fashion, unlike the incremental basis of the first static test. The cradle sustained a maximum applied load of 45 kips without additonal damage. However, a significant amount of plastic bending deformation was observed in the aluminum plate. Contact between the lengthwise edge of the aluminum plate and the U-wall ceased as the aluminum plate deflected. Inspection of the strain data revealed an overloaded condition of the V-wall. The peak V-wall strain was approximately 8000 microstrains in compression at gage #7 while the adjacent U-wall strain at gage #18 was 100 microstrains in tension. A negligible improvement in obtaining symmetric strain readings was realized due to the loading distribution effect of the aluminum plate. It was realistically apparent that a flat endplate configuration would not transfer the recoil rod force, P_r, to the cradle body without experiencing flexural deformation, and producing transverse normal tensile stresses in the adjacent adhesive bond layer.

Static Test #3

A final static test was performed to verify the internal strain distribution capability of the cradle under a uniform load. The recoil rod force, P_r, was applied to the entire surface of the front endplate as a uniformly distributed load to prevent flexural deflection. This type of loading is commonly referred to as platen loading. Dimensional variations were detected over the surface of the front endplate. The endplate surface was subsequently ground flat to alleviate any parallelism discrepancies within ± 0.020". These particular variations were not as detrimental in the previous concentrated load tests. However, such variations would significantly effect the symmetry of strain readings in the platen loaded test. Seventeen new uniaxial strain gages were bonded to the U-wall and V-wall including one gage centered on the top flange of each channel. Previously used gages were damaged during the machining operation of the endplate. Furthermore, since cyclic fatigue loading was to follow after completion of the static tests, the new gages were adhered using BLH EPY-150™ epoxy. This particular epoxy was more suitable for long-term applications. A location map of the new strain gages is shown in Figure 9. The cradle was then successfully platen loaded in compression to 40 kips. Inspection of the strain data revealed that the U-wall and V-wall sustained a maximum compressive strain of 1350 microstrains (gage D) and 1550 microstrains (gage C), respectively. Although the V-wall remained subjected to a 15% overload, a substantial improvement of strain distribution between the U-wall and V-wall was realized. The 15% overload effect existing in the vicinity of the front endplate reduced along the length of the cradle toward the opposite end primarily because of load sharing mechanisms between components other than the U-wall and V-wall; i.e., channels, tubes, and bulkhead. Strain versus load graphs are shown in Figures 10 through 13. Under platen loading conditions, the U-wall and V-wall behaved as desired.

Cyclic Fatigue Test

Fatigue loading of the first sublength cradle was performed to determine the structural response of the cradle to simulated dynamic firing conditions. The applied dynamic force was equivalent to the maximum firing load experienced by an existing M-102 Howitzer. The force versus time relationship for a load pulse simulating live firing is shown in Figure 14. A total of 20,000 cycles with a load amplitude of 25 kips was to be applied. This was representative of one M-102 Howitzer lifetime.

A description of the load pulse was as follows:

The 25 kip load was applied within 30 milliseconds, maintained for 0.1 seconds and then released within 30 milliseconds. This pattern was repeated every 10 seconds. The same platen loaded configuration was employed in the fatigue test as in the #3 static test. Testing was performed using an MTS 100 kip, servo-hydraulic fatigue machine, as shown in Figure 15. The strain gages used in the static test #3 were monitored with the MEGADAC™ system for the fatigue case. Metal shims were positioned between the upper platen and the graphite endplate to compensate for any remaining dimensional variations. The cradle successfully withstood 20,000 cycles of pulsed platen loading without any incident of failure. Strain values of symmetrical gages were reasonably consistent. Strains throughout the cradle were below 900 microstrains in compression. The peak strain response for a particular gage is plotted in Figure 16. Axial displacement of the cradle assembly was measured to be 0.025" at peak load.

Revised Front End Design

An improved front end design was developed which utilizes the in-plane rather than flexural stiffness of the composite material and is shown in Figures 17 and 18. The design consists of four quasi-isotropic graphite/epoxy plates, a front and rear bearing plate, and two parallel support plates. Load transfer from the front bearing plate to the cradle body was optimized by loading the support plates in-plane. An additional enhancement included the slotted holes located adjacent to the bottom edge of each support plate. The function of these holes is to force the load distribution between the support plates and rear bearing plate to occur locally over the regions of the cradle body tubes.

A preliminary static compression test was conducted on the new front end design separately. A 1.25" diameter bolt was positioned in the recoil rod hole of the front end assembly to simulate the presence of the recoil rod nut, as shown in Figure 1b. The assembly was loaded between the platens of a tension/compression machine. Loads from the upper platen were transferred through the bolt head to the front end assembly and reacted by the lower platen. Results of the test indicated the design to be highly successful. An ultimate load of 59 kips was obtained with failure induced by localized ply delaminations along the bottom edges of the support plates, as shown in Figure 19. The mechanics inducing these delaminations were directly attributed to both fiber buckling and transverse normal tensile stresses. At a load level of 54.7 kips, the maximum in-plane deflection was 0.048". Additional tests of the new front end component will be conducted on future prototype cradles.

Elevation Bracket Assembly

The full scale prototype composite cradle design includes elevation rod attachment points which consist of the bracket/plug assemblies, as shown in Figure 2. These assemblies are used to transfer the static reactions and a portion of the dynamic firing loads (see Figure 5) from the cradle through the elevation rods and ultimately to the trails. The elevation brackets were hand laid up, 0.120" thick shells fabricated from Owens Corning™ $0^{o}/90^{o}$ woven S-glass prepreg. Machined aluminum 6061-T6 plugs were bolted to the outside channel web surfaces to provide a means for attaching the elevation rods to the cradle. Three flush head, grade #8, 3/8" diameter bolts were used for each elevation plug. The brackets were adhered to the plugs and cradle by using FM97 epoxy film adhesive. Specifically, the elevation brackets served two purposes:

- The elevation brackets were designed to transfer a portion of the loads from the upper flanges of the channels and cradle side walls to the plugs. The remainder of the applied loading was supported by the 3/8" diameter bolts used to secure the plugs to the channel webs. This eliminated potential overloading effects on these critical fasteners.
- The design maximized the use of available bonding area between the brackets and cradle side walls. Several 1/4" diameter fasteners were also installed along the flange surfaces of the brackets to minimize adhesive peel stresses in critical areas. These fastener locations are shown in Figure 2.

Static testing of the elevation bracket/plug assemblies was performed in conjunction with a sublength cradle. The maximum working load on a per bracket/plug assembly basis was determined by actual field firing tests to be 3300 lbs. at 33^{o} (with respect to the recoil rod axis). A factor of safety of 2.0 was imposed on these attachments thus raising the design load to 6600 lbs. per bracket/plug assembly. A hydraulic test frame consisting of one 20 kip actuator and a Y-shaped ram was used to load both elevation bracket/plug assemblies simultaneously. The sublength cradle incorporating these assemblies was successfully loaded to the maximum actuator load, 20 kips, without any indication of failure.

Trunnion Joint

The majority of the recoil load is reacted by two trunnion joints located at the rearward end of the cradle (see Figure 2). These joints are used to attach the cradle to the trails. Maximum trunnion reactions were measured during the ARDEC field firing tests. The magnitude of these reactions was 12 kips per trunnion. The primary loading vector, P_r, was determined to be parallel and collinear with the outer surfaces of the channel flanges. This was confirmed by strain measurements taken during the ARDEC live firing tests and applies only for the section of the cradle located beyond the elevation brackets toward the trunnion end. Using a safety factor equal to 1.5, the trunnion joint design load was calculated at 18 kips.

The composite cradle design includes machined, S-glass trunnion doublers bonded and fastened to each side of the cradle. Loads are to be distributed from the cradle body to the two trunnion joints resulting in a double shear mode loading configuration. However, since the load path is eccentric from the cradle body to the trunnions, out-of-plane bending moments were expected to exist within these joints. Consequently, peel stresses would also develop along the vertical edges of the trunnion doubler bond lines. Tapering of these edges for purposes of alleviating peel stresses was not practical since the doublers were relatively thick.[5] However, the trunnion fasteners served two purposes: First, the existing aluminum trunnion brackets, which are part of the trails and not the cradle, must be secured in position to the S-glass doublers with mechanical fasteners. These fasteners allow for cradle installation and removal. Secondly, the fasteners reduce the eccentricity effects or, more specifically, the peel stress on the adhesive bond layer between the trunnion doubler and cradle body.

Testing of the sublength composite cradle incorporating a proposed trunnion joint design was not performed during this evaluation. Additional analytical, experimental, and design related activities were necessary to determine the optimum joint geometry and load transfer mechanisms. Furthermore, this was a difficult task to complete without empirical test data

5. DOD/NASA Advanced Composites Design Guide. Air Force Wright Aeronautical Laboratories. v 1-A. Design. 1st Edition. 1983.

since strength of materials bolt load distribution theories apply to ductile materials only and do not apply to the brittle composite materials[5] used in the cradle. However, current efforts investigated the response of a generic, mechanically fastened, and adhesively bonded joint subject to an eccentric load. The generic joint which incorporated an aluminum loading plate, S-glass doubler, and graphite/epoxy channel specimen was designed and tested to quantify the distribution of applied loads to individual fasteners. This test was not conducted to simulate a prototype trunnion joint, however, but rather to generate empirical load versus strain data for a generic configuration consisting of the same material system. The geometry of this test specimen is described in Figure 20.

Assembly of the test specimen was as follows:

> Four matching, 1/2" diameter countersunk holes were simultaneously drilled through the web of a 5.50" long graphite/epoxy channel section, a 1.00" thick $0^{o}/90^{o}$ woven S-glass doubler, and a 0.07" thick 4340 steel washer plate. A sufficient piece of FM97 film adhesive was then positioned on the outer web surface of the channel so that the corresponding bolt hole locations could be cut out. This adhesive layer was to be used for attaching the channel to the doubler. After the manufacturer's recommended surface preparation was performed, the film adhesive was fitted between the outer channel web and adjacent doubler surfaces. A 0.50" thick aluminum 6061-T6 plate, four 1/2" diameter grade #8 flush head fasteners, and steel washer plate were then installed. The washer plate served two purposes: (1) it represented the bearing strips used in the channel section of the aluminum cradle, and (2) it would prevent potential fastener bearing or pull-through failures in the graphite/epoxy channel. The test specimen was then cured according to manufacturer specifications upon complete assembly. Strain gages were later positioned at various locations to measure local bypass and extensional strains.

The preliminary trunnion joint test specimen was loaded using an electro-mechanical, 50 kip Instron™ test machine. The single shear loading diagram (see Figure 21) shows the aluminum plate secured in the top wedge grip and the bottom surface of only the graphite/epoxy channel reacting on the lower platen. The doubler thickness was calculated to ensure that the amount of load path eccentricity found in the aluminum cradle was equivalent to that of the generic joint. A flat piece of wood was positioned between the bottom surface of the channel and the platen to provide a near uniform load distribution over the channel cross section. The fasteners were torqued to 1600 in./lbs. Concern was raised regarding possible damage to the Instron™ load cells due to the eccentric load path existing within the joint specimen. (Typically, axial load cells must be designed to withstand some prescribed amount of off-axis loading; however, exceeding this amount will cause permanent damage to the load cell.) In order to determine such eccentricity and prevent damage to the load cell during testing, two strain gages were positioned on the faces of the aluminum plate, as shown in Figure 21. These gages were connected to X-Y recorders for real-time monitoring. Bending strains from these two gages would be used by test engineers to monitor the amount of eccentric moment reacted through the load cell. All other strain gages were mounted on the graphite/epoxy channel and read using the OPTILOG™ data acquisition system.

The first series of loading cycles was conducted at a crosshead speed of 0.05" per minute. Four compressive load cycles with peak magnitudes of 4 kips were applied. All gages located on the channel section indicated compressive strains under 300 microstrains. There were no observable bending deformation or recorded plastic strains in the gages on the aluminum plate.

An additional cycle was applied in anticipation of loading the joint to failure. Strength of materials calculations estimated the load required to yield the aluminum plate to be approximately 3000 lbs. The test was terminated at 5250 lbs. when visual inspection of the aluminum plate revealed the presence of a plastic hinge at the plate/grip interface. At 5250 lbs. all channel section strain gages read below 400 microstrains in compression.

The 0.50" thick aluminum loading plate was replaced with a 1.00" thick aluminum plate. The two-to-one increase in plate thickness resulted in an overall bending stiffness (E x I) increase of eight-to-one. A final load cycle was applied at a crosshead speed of 0.20" per minute. The added stiffness allowed the test specimen to be loaded successfully to 20 kips without any incident of failure. However, the maximum eccentric load capacity of the Instron™ load cell was reached. Extensional and bypass strains for the 20 kip cycle are shown in Figure 21.

CONCLUSIONS

Initial structural evaluation efforts for the first sublength composite M-102 cradle body were completed. Loads applied during the cradle body tests were restricted to simulated recoil type loads. Secondary loads and reactions were not included in the current effort. Static tests #1 and #2 revealed that a flat endplate design was incapable of (1) uniformly distributing a recoil load to the cradle body, and (2) preventing the development of transverse normal tensile stresses within adjacent adhesive layers. However, the idealized platen loading configuration used in static test #3 demonstrated axial cradle body strains in the order 0.15% at a peak load of 40 kips. Furthermore, because the axial strains were relatively low in comparison to those obtained in the compression coupon tests, additional weight reductions will be attainable. Thickness reductions of the various thin-walled components will be considered for future prototypes once an effective front endplate design is incorporated. Static test #3 exhibited comparable strains at symmetrically located gages once dimensional variations were reduced along the front endplate surface. The maximum variation in loading between the U-wall and V-wall during this test was 15%.

The fatigue test, employing a platen loaded configuration, was highly successful. The sublength prototype survived 20,000 cycles of simulated firing without damage. All axial strains measured at discrete locations were below 900 microstrains in compression. There were no indications of Euler or localized plate buckling in any of these tests.

Static tests #1 and #2 revealed several problems originating from the cradle manufacturing processes. Dimensional stability of the composite cradle was not maintained. Inspection of the individual components and the assembled cradle body revealed that dimensions were out-of-tolerance due to such factors as (1) improper machining, (2) thermal expansion of the aluminum molds at manufacturer specified curing temperatures, and (3) residual curing stresses within the composite materials. These factors contributed to the unsymmetrical strain distributions exhibited during testing.

A revised front end concept was developed which relied upon the in-plane rather than flexural stiffness of the graphite/epoxy material to transfer the recoil load from the recoil rod to the cradle body. This design proved highly successful during individual component tests by achieving an ultimate load of 59 kips. Structural responses of the front end component resulting from the platen reacted test described herein and future cradle body reacted tests are expected to be identical. This is justified because the localized transfer of recoil forces through the outer regions of the front end assembly is independent of the supporting foundation stiffness. In light of the 45 kip design load (factor of safety included), an excessive strength margin of 31% was exhibited. Therefore, development of a lighter weight front end component will be investigated and incorporated in future prototype cradle tests.

The elevation bracket/plug design was completed and successfully tested without failure to loads 52% greater than that required. Testing ceased once the applied load reached the limits of the hydraulic actuator system. Load sharing between the adjacent adhesive layers prevented overloading of the mechanical fasteners used to secure the plugs to the channels as intended. The optimized bracket/plug assembly, as shown in Figure 17, was developed to provide weight reductions based upon the 52% excessive strength margin. Design revisions include a hollowed out plug and shortened bracket component and will be evaluated in future prototypes. Additional weight reductions may be performed once the ultimate strength of the bracket/plug assembly is determined from testing.

A preliminary test was conducted on an eccentrically loaded, mechanically fastened graphite/epoxy channel to determine individual fastener loads in brittle composite materials. The resulting strain data will assist in determining the optimum bolt pattern for use in the trunnion joint design. In all likelihood, the trunnion joint would include an adhesive layer and approximately six to eight mechanical fasteners installed through the channel and U-wall skin, as shown in Figure 22. The loading frame of Figure 22 will be used for structural evaluation of trunnion joints in conjunction with both sublength and full scale prototype cradles.

ACKNOWLEDGMENTS

The MTL Lightweight Howitzer (LWH) Program combines the strengths and resources of various inhouse laboratories, management, and support functions. Only through the cooperation of these groups has the LWH team accomplished the goals that were set forth. Special recognition and appreciation is given to T. Blanas and G. Libby for their assistance in fabricating the composite cradle components. The authors are indebted to C. Cavallaro, P. Benton, R. Dooley, and C. DiBona for their assistance in strain gaging and instrumentation monitoring. Ackowledgment is also given to N. Lionetti, R. Becker, and H. Liberman of the ARDEC's Future Weapons Branch for their continued interest and support, as well as providing technical information and consultation.

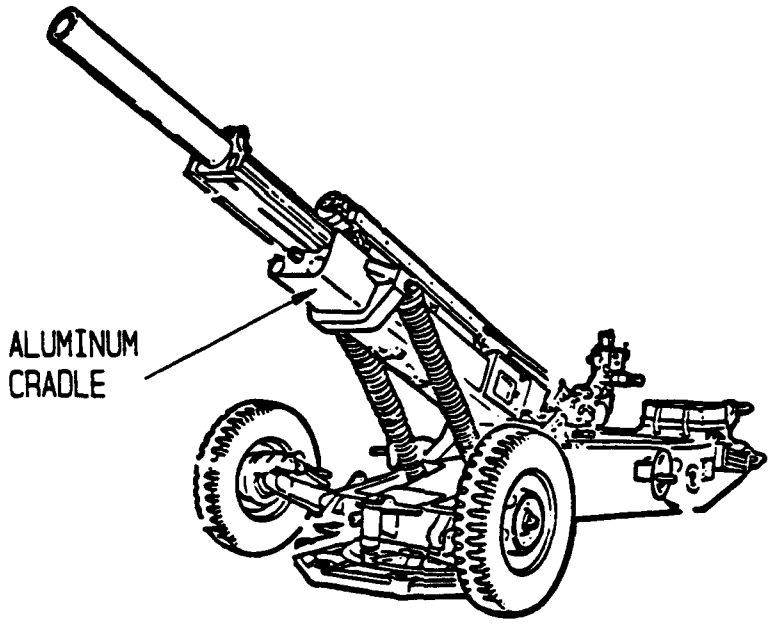

Figure 1a. M-102 towed Howitzer.

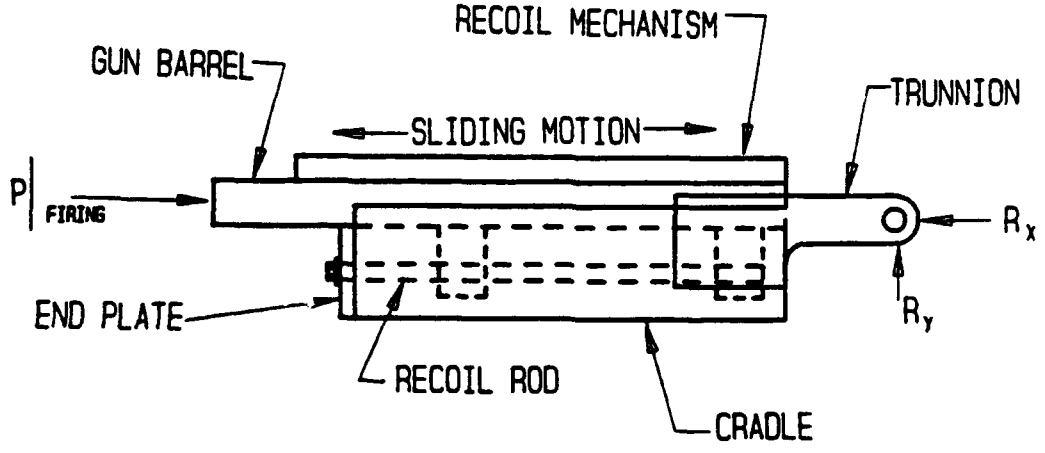

Figure 1b. Recoil rod reactions.

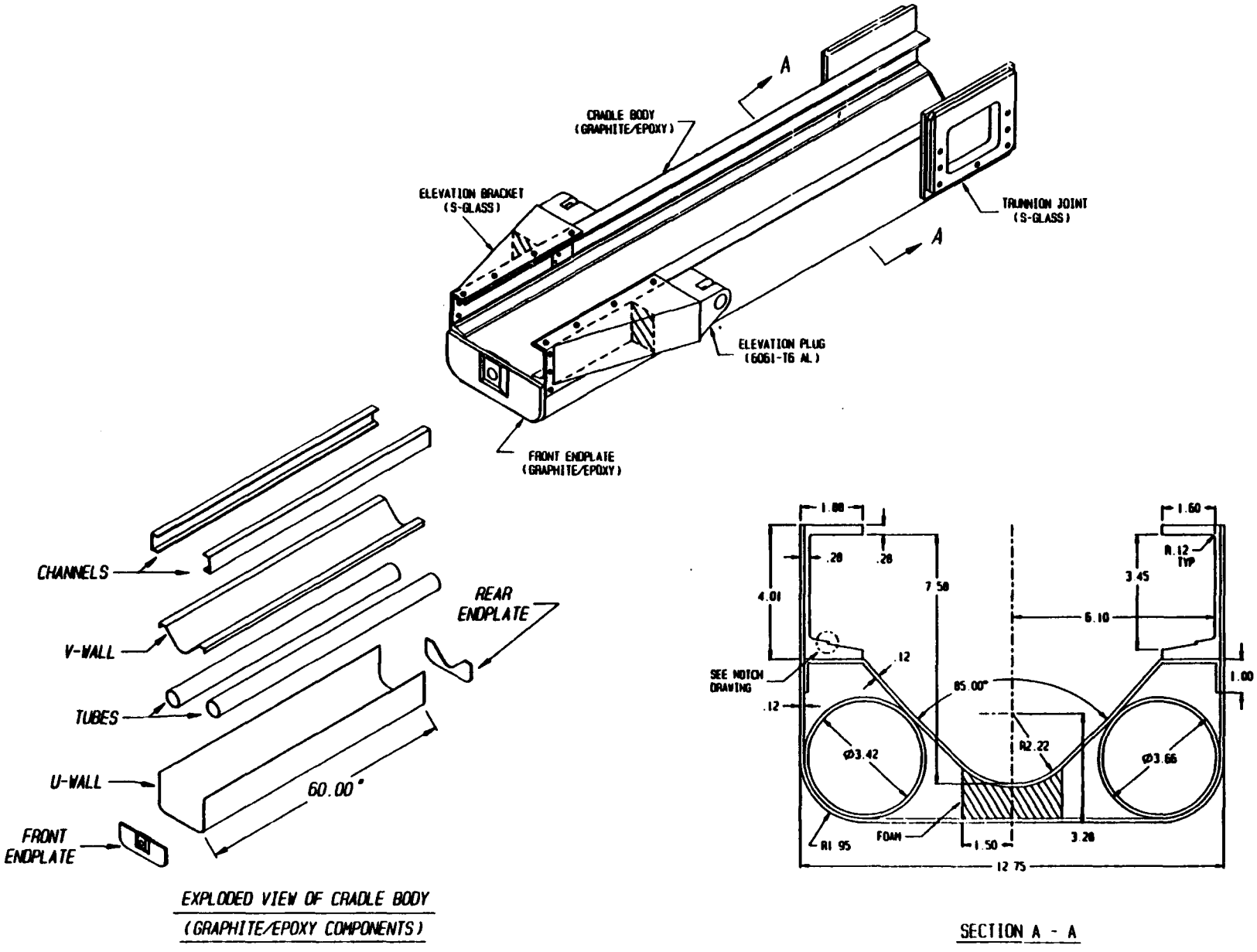

Figure 2. MTL composite cradle design.

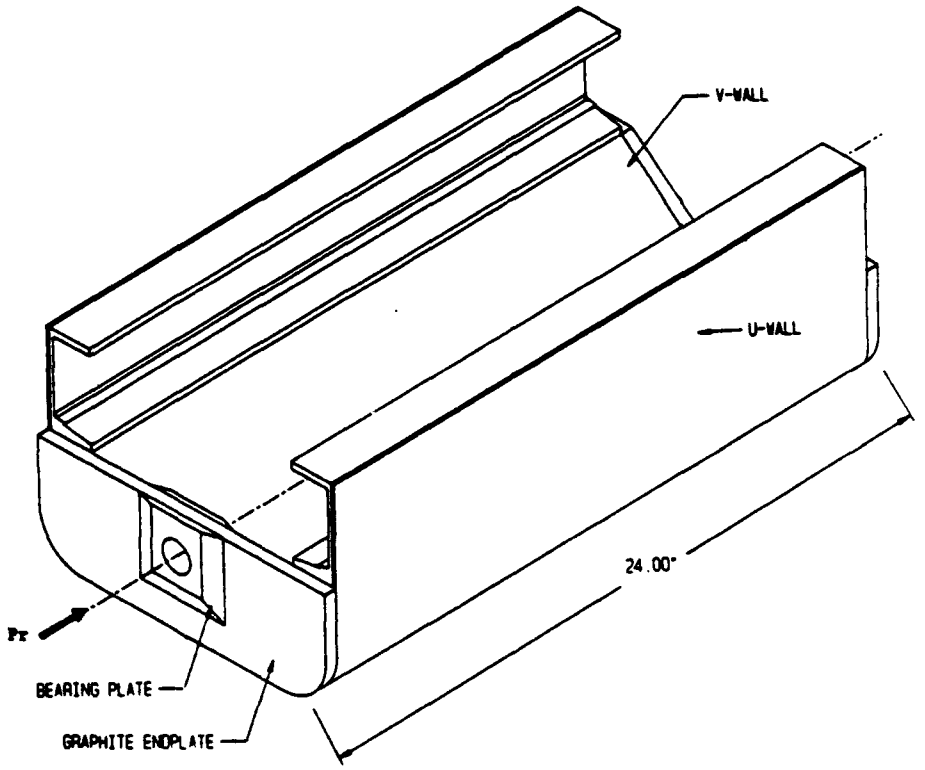

Figure 3. MTL sublength composite cradle.

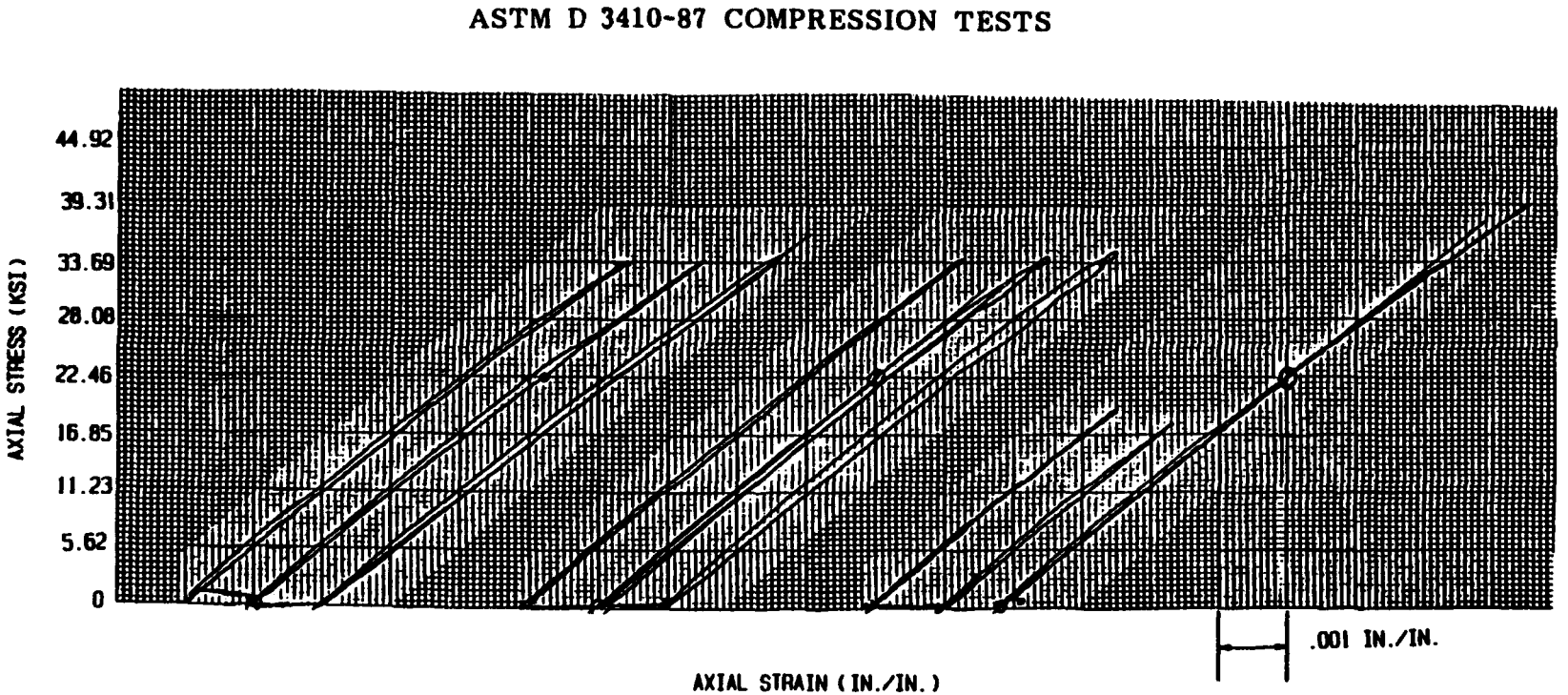

Figure 4. Compressive stress-strain curves for fiberite GR/EP prepreg.

FIRING LOADS AND REACTIONS ON M-102 CRADLE			
Elevation Angle	0°	45°	75°
(recoil length)	(long)	(short)	(short)
TX	11,300	12,300	4,467
TY	1,458	13,300	17,744
EX	2,693	631	78
EY	1,274	1,758	1,306
V2b	144	1,049	1,427
V2s	6,035	---	---
V21	---	2,902	3,042
Pr	11,200	18,700	18,500
(Loads in Lbs.)			
SUFFIXES			
x,y - Horizontal and Vertical Coordinate			
b - Battery Position			
l - Long Recoil			
s - Short Recoil			

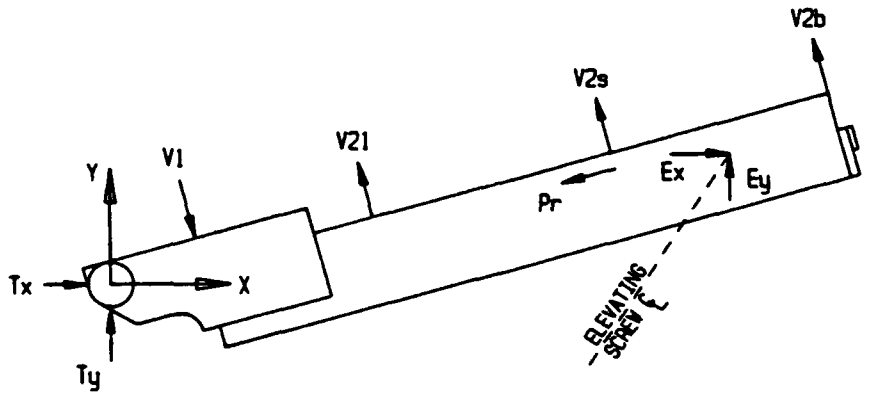

Figure 5. Aluminum cradle loading diagram.

TEST TYPE	LOADING	RESULTS
#1 Static	Concentrated load applied to graphite.	Graphite endplate debonded from cradle at 10% required load.
#2 Static	Concentrated load applied to 1" thick Al 6061-T6 plate on top of graphite endplate.	Significant plastic bending deformation of aluminum plate. Max load = 45 kips No damage to cradle.
#3 Static	Platen loading	Max load = 40 kips No damage evident.
#4 Fatigue	Platen loading	Cradle withstood 20,000 cycles of simulated firing. Max load = 25 kips. No damage evident.

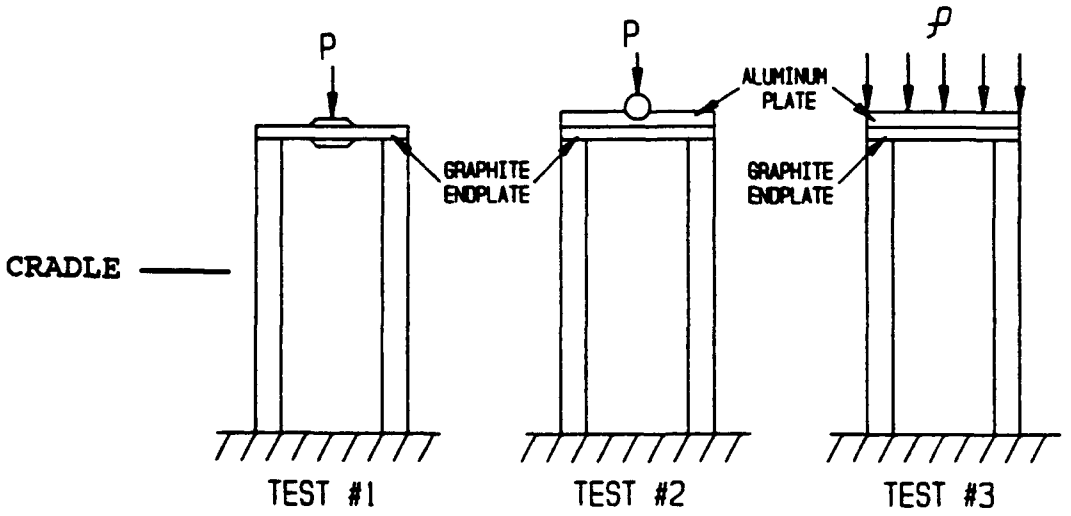

Figure 6. Structural test configurations and results.

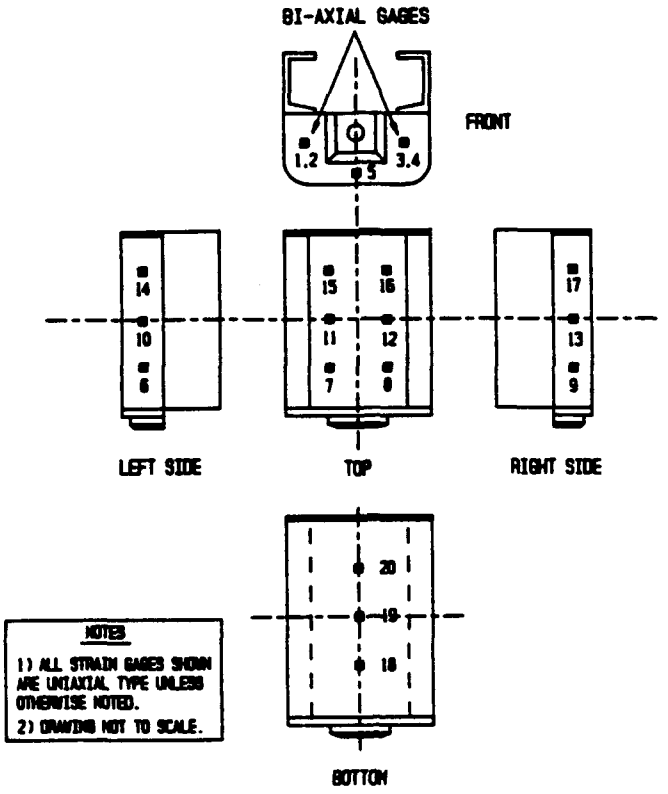

Figure 7. Strain gage location map - static tests #1 and #2.

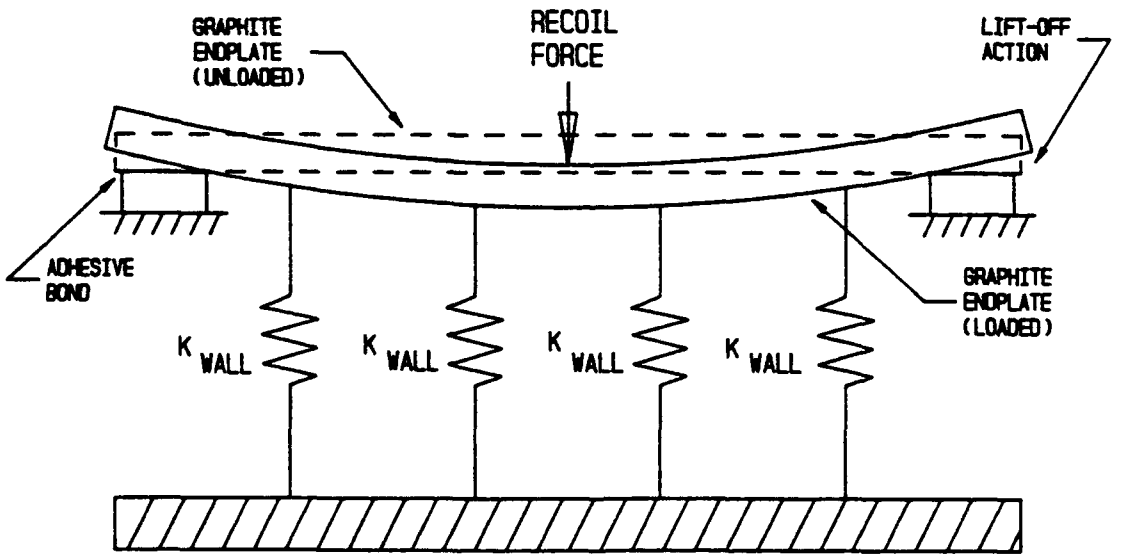

- SPRINGS REPRESENT INNER & OUTER WALL EDGES OF CRADLE

WHERE: $K_{WALLS} >> E \times I_{ENDPLATE}$

Figure 8. Beam/spring endplate model.

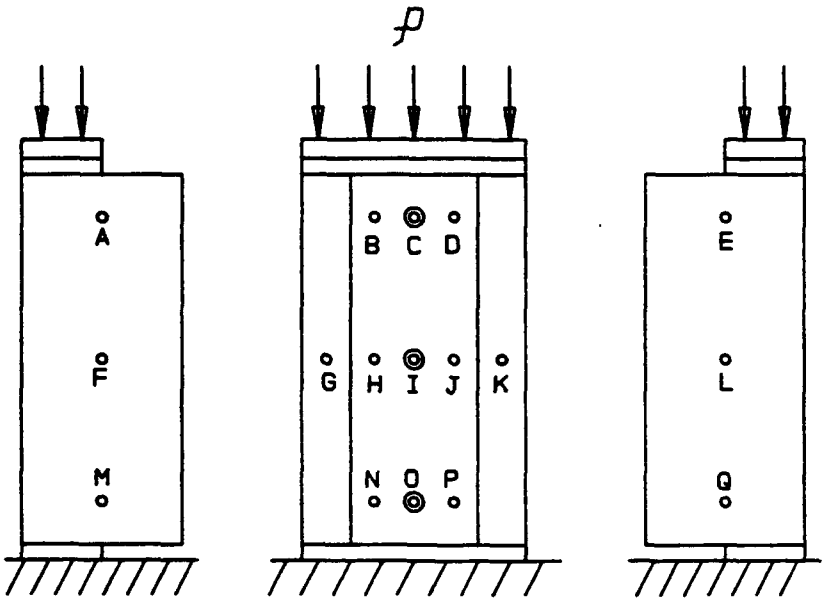

Figure 9. Strain gage location map - static test #3, fatigue test.

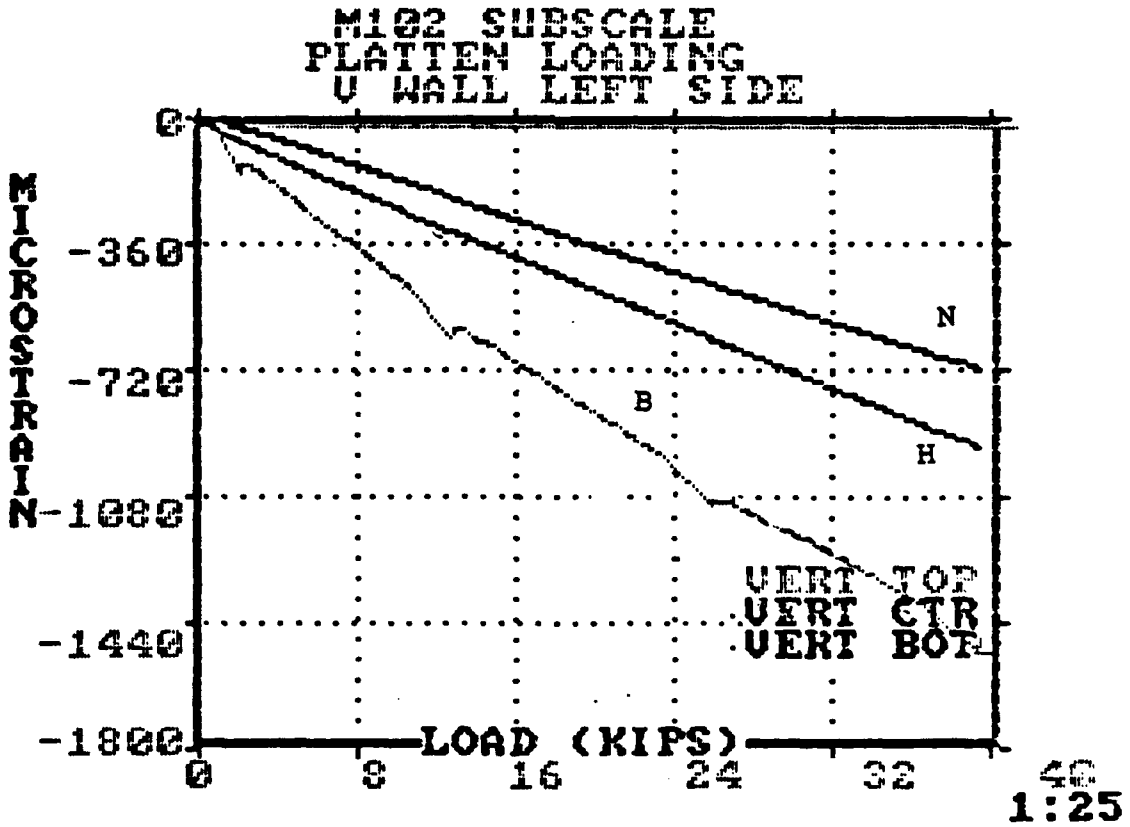

Figure 10. Platen test strain versus load curves.

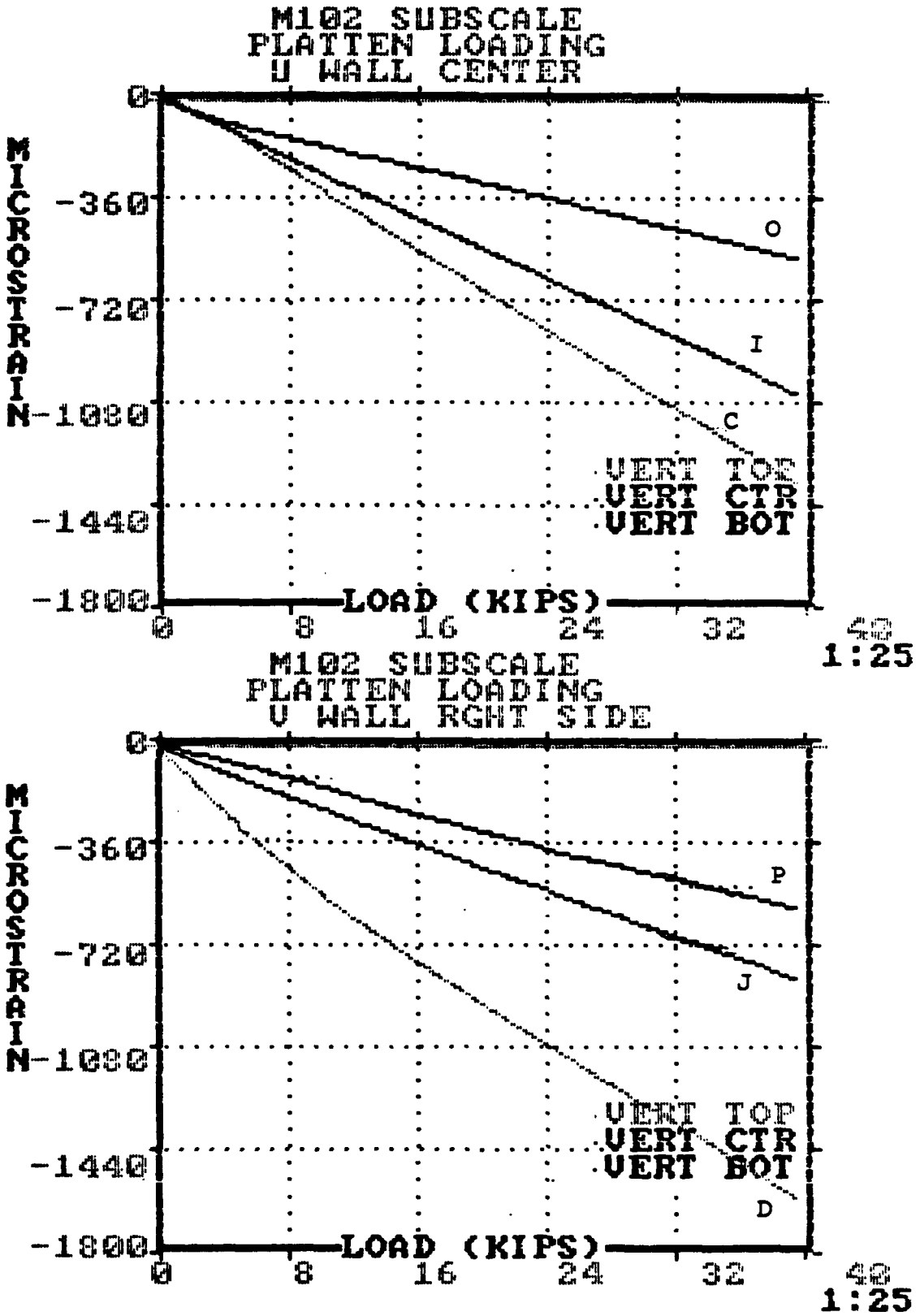

Figure 11. Platen test strain versus load curves.

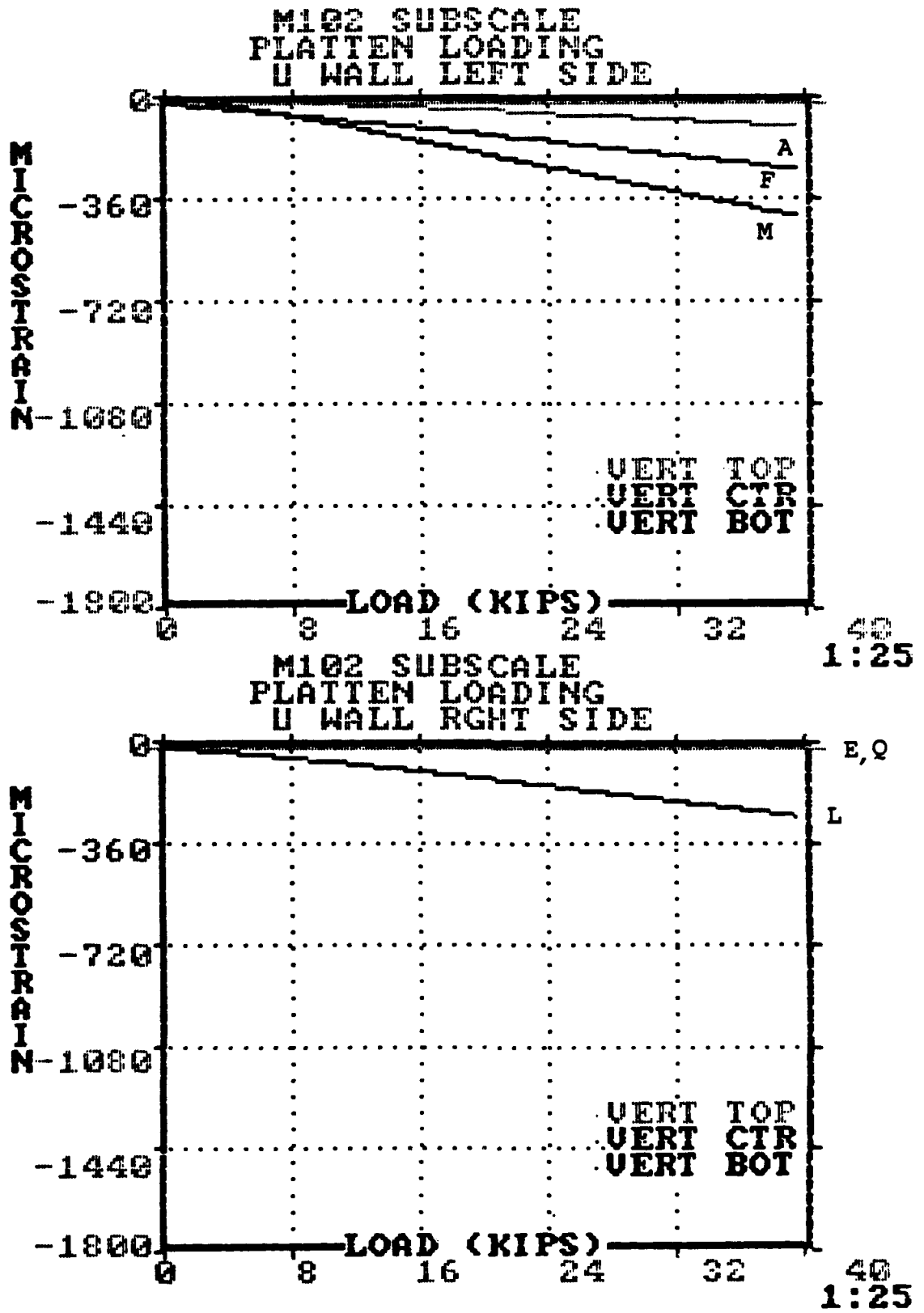

Figure 12. Platen test strain versus load curves.

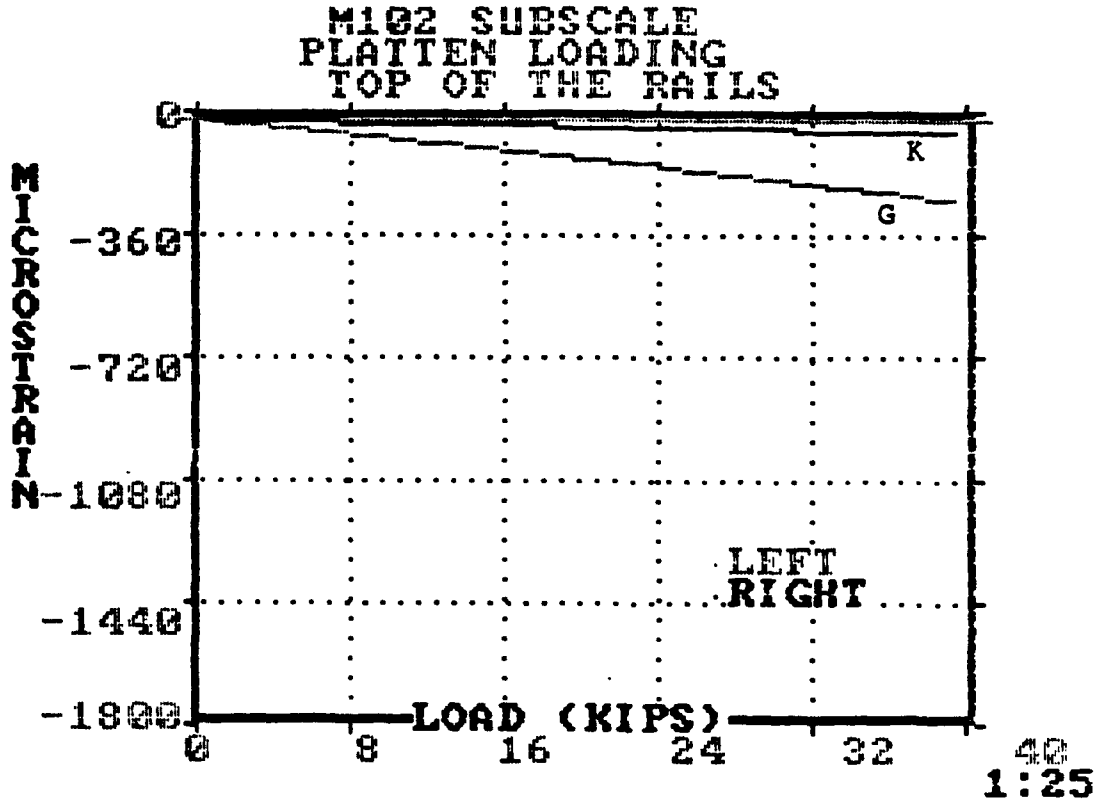

Figure 13. Platen test strain versus load curves.

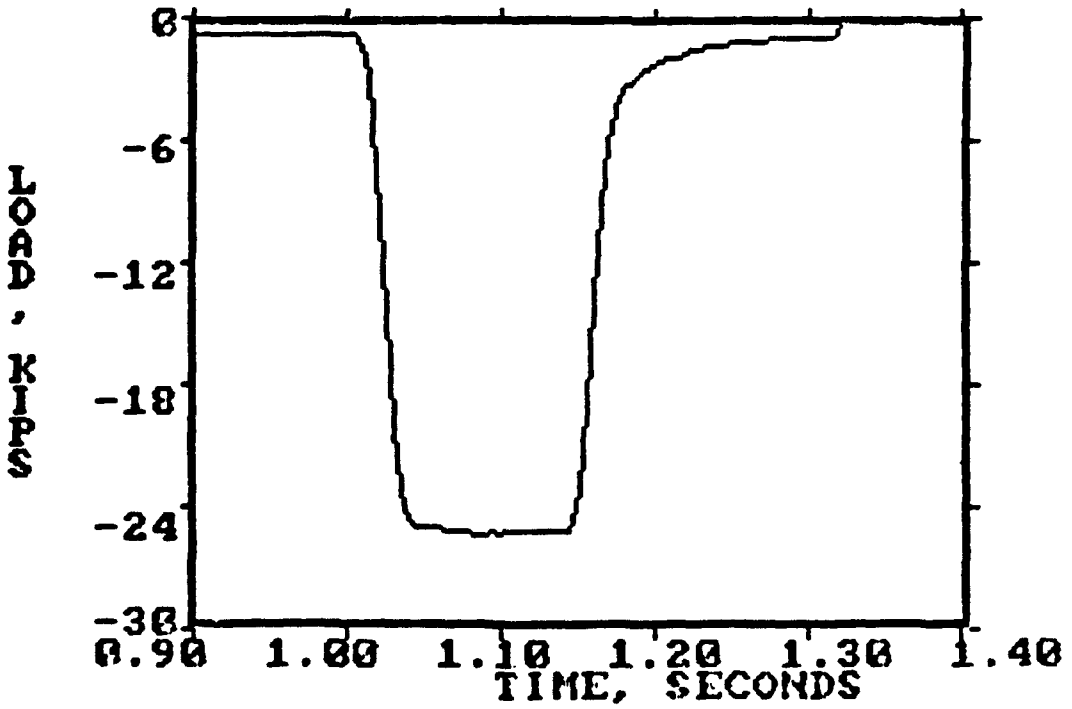

Figure 14. Dynamic load pulse definition.

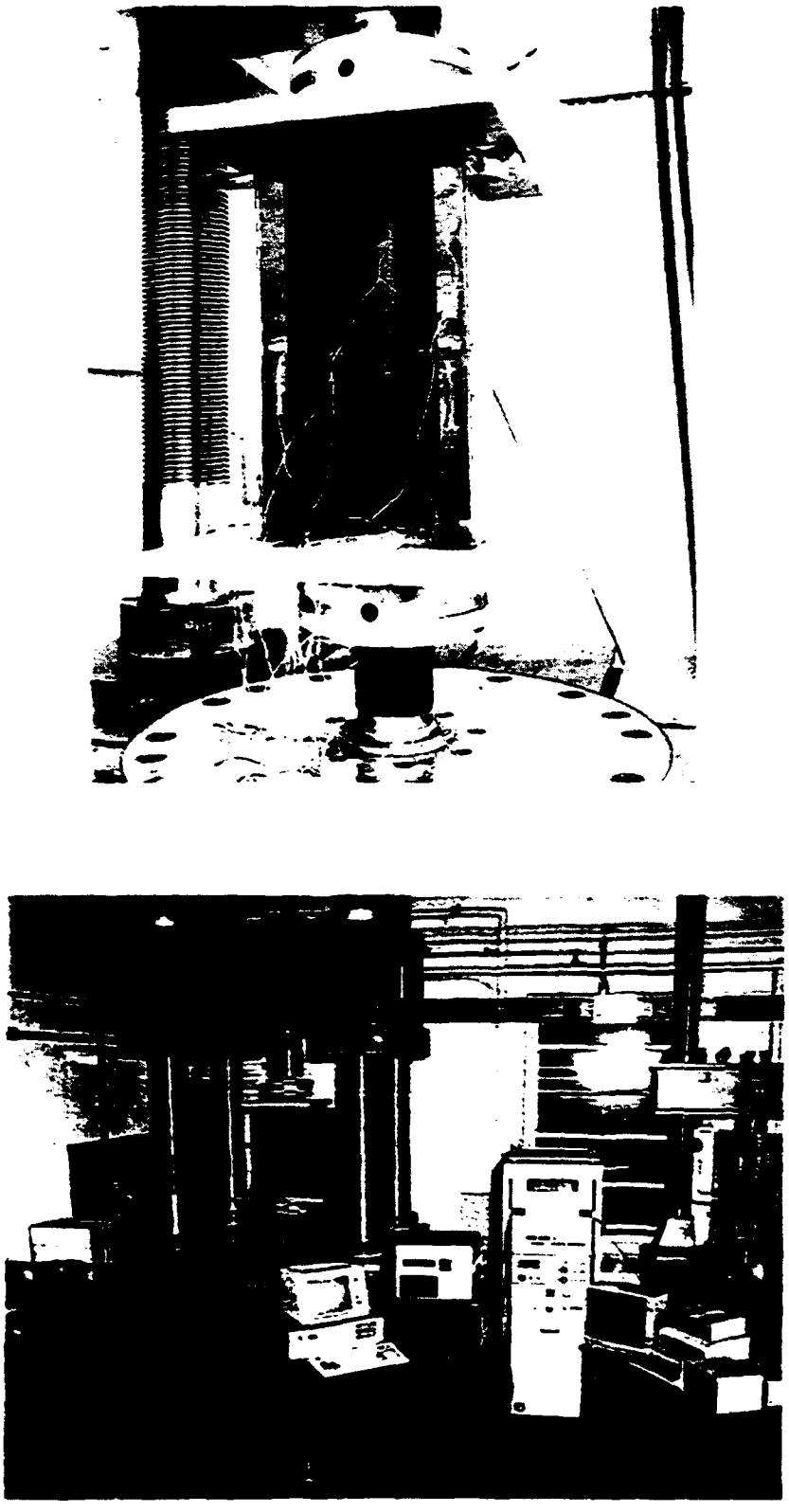

Figure 15. Dynamic fatigue test apparatus.

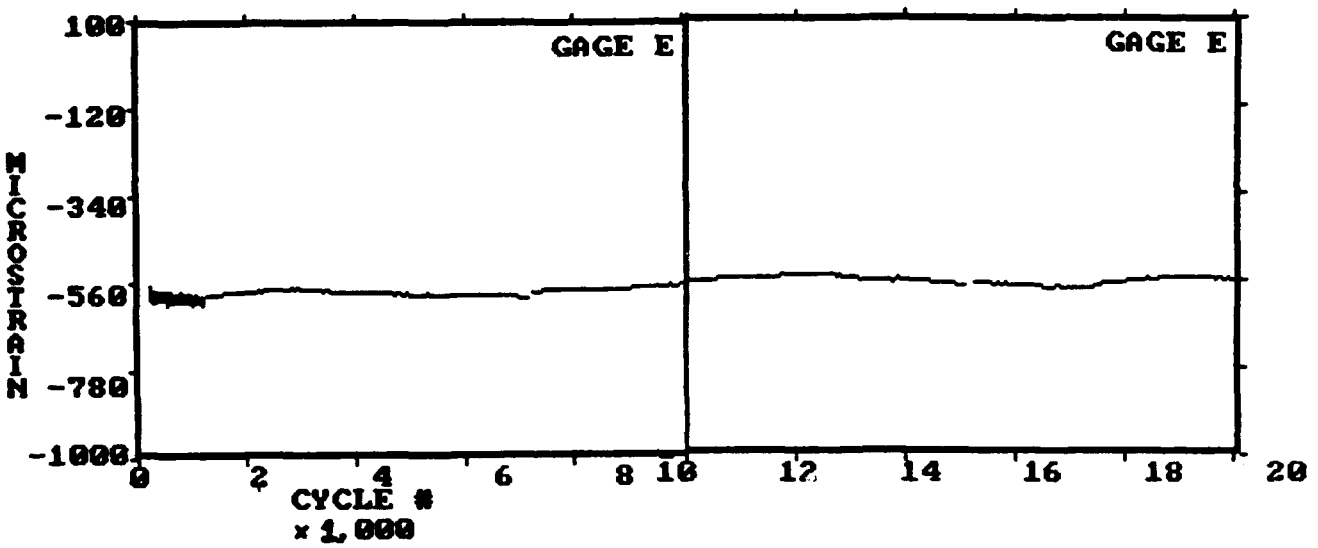

Figure 16. Strain history curve.

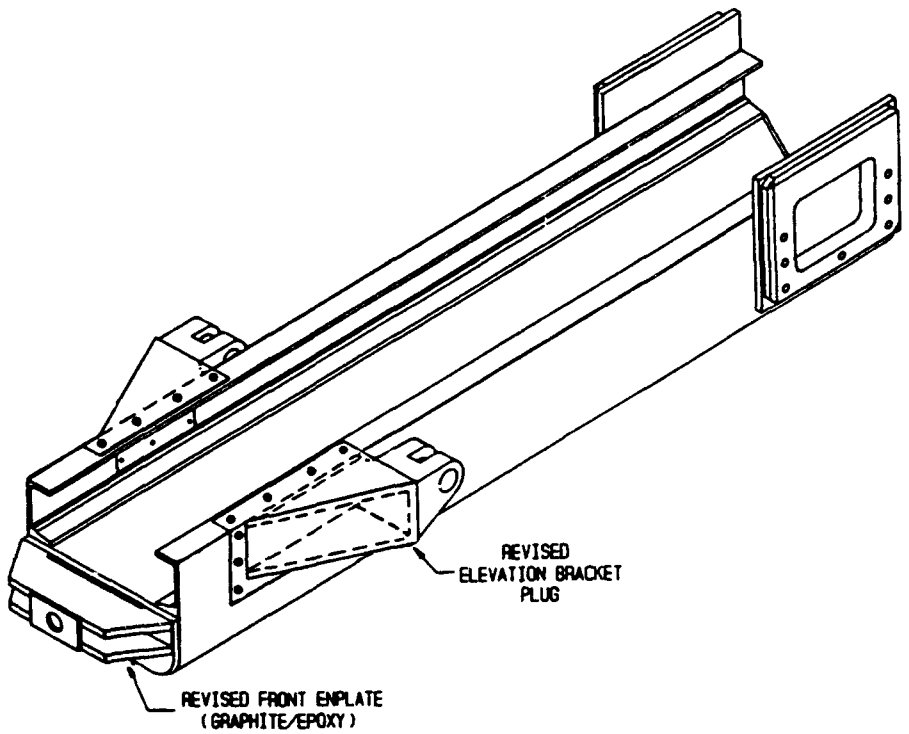

Figure 17. Revised front end design and elevation bracket-plug assembly.

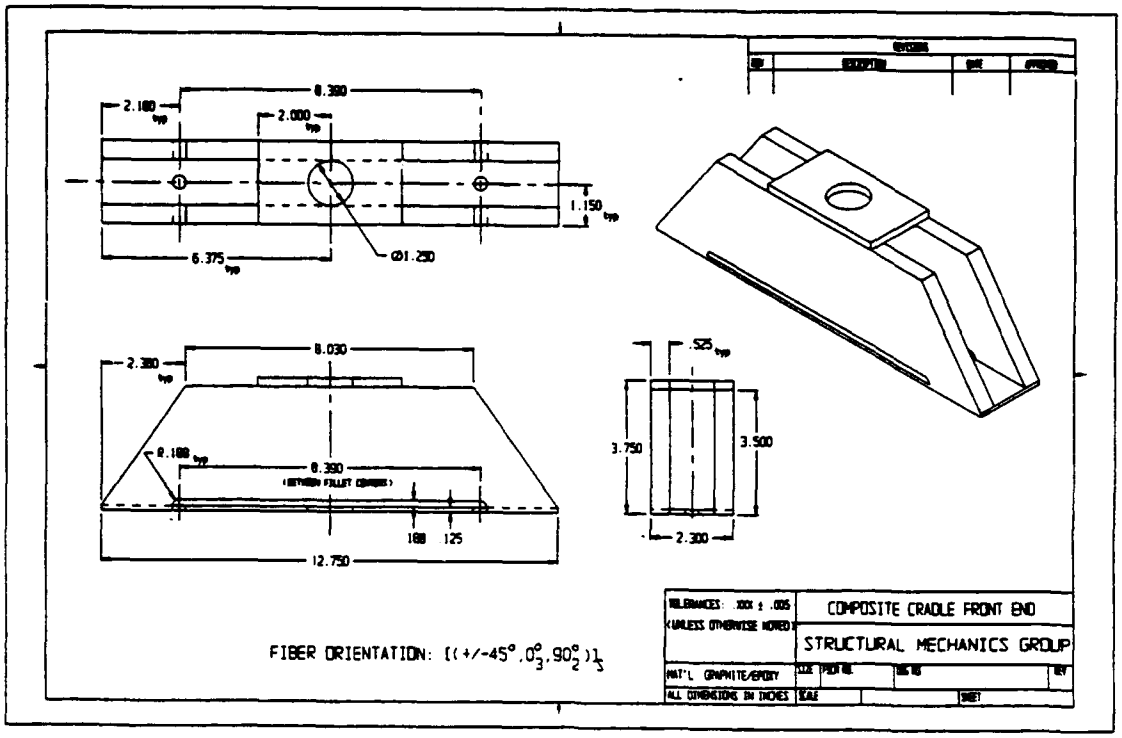

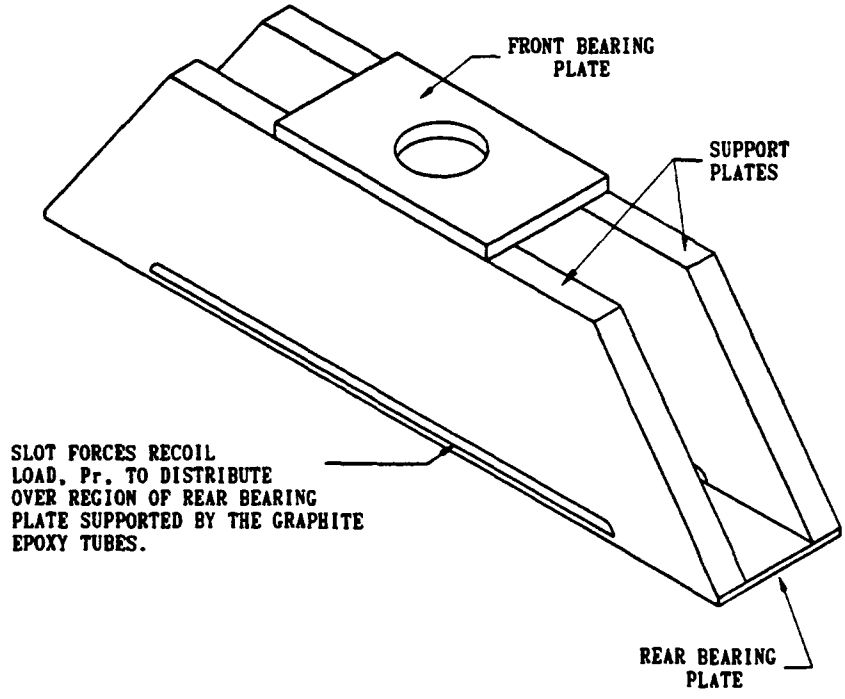

Figure 18. Revised front end design.

Figure 19. Failure mode for revised front end.

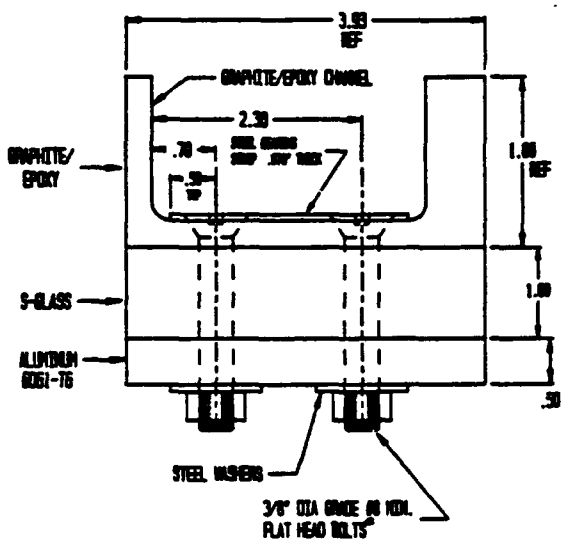

End view

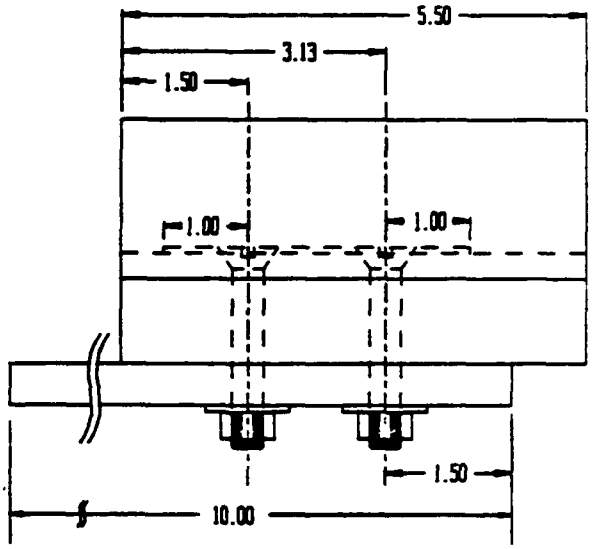

Side view

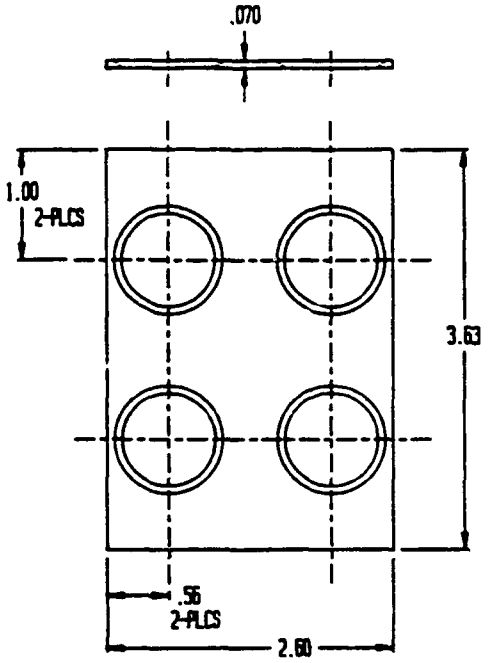

Steel bearing strip

Figure 20. Preliminary trunnion joint test specimen.

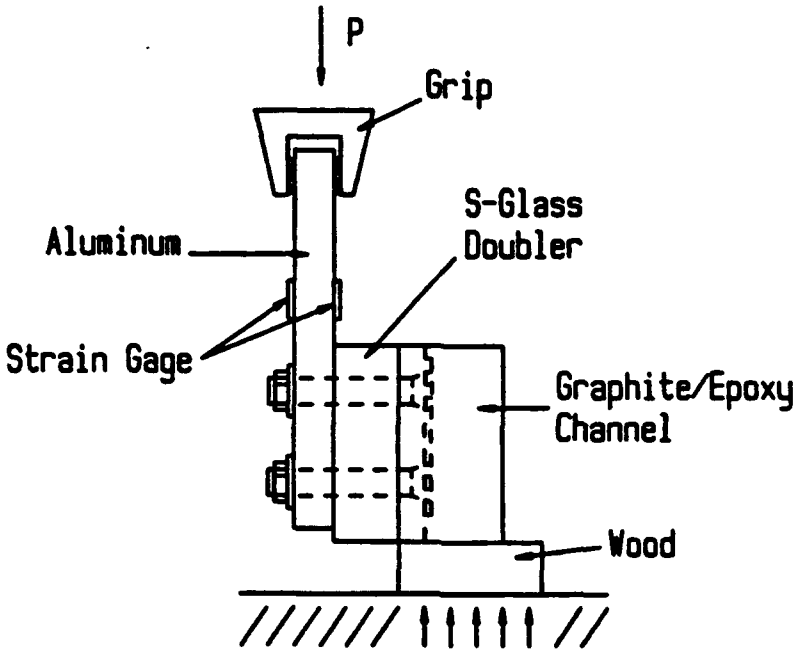

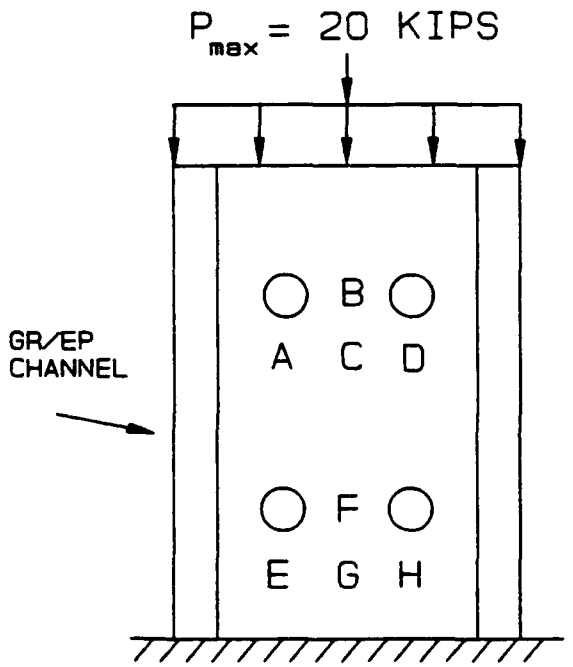

GAGE	STRAIN*
A	-1450
B	-779
C	-1399
D	-1325
E	-1319
F	-1121
G	N/A
H	-1097

* - MICRO INCHES / INCH

Figure 21. Loading configuration and strain data.

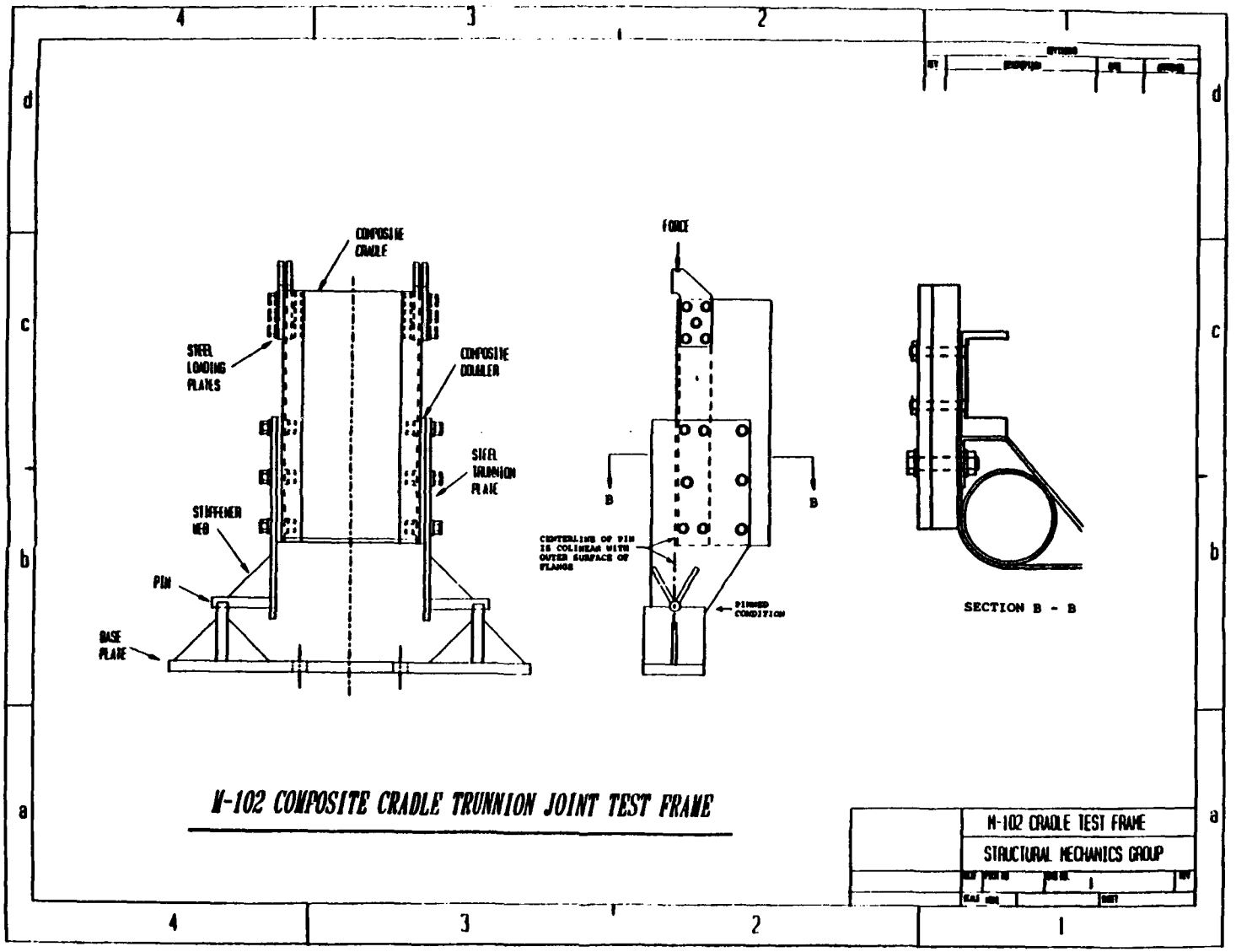

Figure 22. Proposed trunnion fastener locations and loading frame.

DISTRIBUTION LIST

No. of Copies	To
1	Office of the Under Secretary of Defense for Research and Engineering, The Pentagon, Washington, DC 20301
	Commander, U.S. Army Laboratory Command, 2800 Powder Mill Road, Adelphi, MD 20783-1145
1	ATTN: AMSLC-IM-TL
1	AMSLC-CT
	Commander, Defense Technical Information Center, Cameron Station, Building 5, 5010 Duke Street, Alexandria, VA 22304-6145
2	ATTN: DTIC-FDAC
1	MIAC/CINDAS, Purdue University, 2595 Yeager Road, West Lafayette, IN 47905
	Commander, Army Research Office, P.O. Box 12211, Research Triangle Park, NC 27709-2211
1	ATTN: Information Processing Office
	Commander, U.S. Army Materiel Command, 5001 Eisenhower Avenue, Alexandria, VA 22333
1	ATTN: AMCSCI
	Commander, U.S. Army Materiel Systems Analysis Activity, Aberdeen Proving Ground, MD 21005
1	ATTN: AMXSY-MP, H. Cohen
	Commander, U.S. Army Missile Command, Redstone Scientific Information Center, Redstone Arsenal, AL 35898-5241
1	ATTN: AMSMI-RD-CS-R/Doc
1	AMSMI-RLM
	Commander, U.S. Army Armament, Munitions and Chemical Command, Dover, NJ 07801
1	ATTN: Technical Library
	Commander, U.S. Army Natick Research, Development and Engineering Center, Natick, MA 01760-5010
1	ATTN: Technical Library
	Commander, U.S. Army Satellite Communications Agency, Fort Monmouth, NJ 07703
1	ATTN: Technical Document Center
	Commander, U.S. Army Tank-Automotive Command, Warren, MI 48397-5000
1	ATTN: AMSTA-ZSK
1	AMSTA-TSL, Technical Library
	Commander, White Sands Missile Range, NM 88002
1	ATTN: STEWS-WS-VT
	President, Airborne, Electronics and Special Warfare Board, Fort Bragg, NC 28307
1	ATTN: Library
	Director, U.S. Army Ballistic Research Laboratory, Aberdeen Proving Ground, MD 21005
1	ATTN: SLCBR-TSB-S (STINFO)
	Commander, Dugway Proving Ground, Dugway, UT 84022
1	ATTN: Technical Library, Technical Information Division
	Commander, Harry Diamond Laboratories, 2800 Powder Mill Road, Adelphi, MD 20783
1	ATTN: Technical Information Office
	Director, Benet Weapons Laboratory, LCWSL, USA AMCCOM, Watervliet, NY 12189
1	ATTN: AMSMC-LCB-TL
1	AMSMC-LCB-R
1	AMSMC-LCB-RM
1	AMSMC-LCB-RP
	Commander, U.S. Army Foreign Science and Technology Center, 220 7th Street, N.E., Charlottesville, VA 22901-5396
3	ATTN: AIFRTC, Applied Technologies Branch, Gerald Schlesinger
1	Plastics Technical Evaluation Center, (PLASTEC), ARDEC, Bldg. 355N, Picatinny Arsenal, NJ 07806-5000
	Commander, U.S. Army Aeromedical Research Unit, P.O. Box 577, Fort Rucker, AL 36360
1	ATTN: Technical Library

No. of Copies	To
	Commander, U.S. Army Aviation Systems Command, Aviation Research and Technology Activity, Aviation Applied Technology Directorate, Fort Eustis, VA 23604-5577
1	ATTN: SAVDL-E-MOS
	U.S. Army Aviation Training Library, Fort Rucker, AL 36360
1	ATTN: Building 5906-5907
	Commander, U.S. Army Agency for Aviation Safety, Fort Rucker, AL 36362
1	ATTN: Technical Library
	Commander, USACDC Air Defense Agency, Fort Bliss, TX 79916
1	ATTN: Technical Library
1	Clarke Engineer School Library, 3202 Nebraska Ave. North, Ft. Leonard Wood, MO 65473-5000
	Commander, U.S. Army Engineer Waterways Experiment Station, P. O. Box 631, Vicksburg, MS 39180
1	ATTN: Research Center Library
	Commandant, U.S. Army Quartermaster School, Fort Lee, VA 23801
1	ATTN: Quartermaster School Library
	Naval Research Laboratory, Washington, DC 20375
1	ATTN: Code 5830
1	Dr. G. R. Yoder - Code 6384
	Chief of Naval Research, Arlington, VA 22217
1	ATTN: Code 471
1	Edward J. Morrissey, WRDC/MLTE, Wright-Patterson Air Force, Base, OH 45433-6523
	Commander, U.S. Air Force Wright Research & Development Center, Wright-Patterson Air Force Base, OH 45433-6523
1	ATTN: WRDC/MLLP, M. Forney, Jr.
1	WRDC/MLBC, Mr. Stanley Schulman
	NASA - Marshall Space Flight Center, MSFC, AL 35812
1	ATTN: Mr. Paul Schuerer/EH01
	U.S. Department of Commerce, National Institute of Standards and Technology, Gaithersburg, MD 20899
1	ATTN: Stephen M. Hsu, Chief, Ceramics Division, Institute for Materials Science and Engineering
1	Committee on Marine Structures, Marine Board, National Research Council, 2101 Constitution Ave., N.W., Washington, DC 20418
1	Librarian, Materials Sciences Corporation, 930 Harvest Drive, Suite 300, Blue Bell, PA 19422
1	The Charles Stark Draper Laboratory, 68 Albany Street, Cambridge, MA 02139
	Wyman-Gordon Company, Worcester, MA 01601
1	ATTN: Technical Library
	General Dynamics, Convair Aerospace Division, P.O. Box 748, Fort Worth, TX 76101
1	ATTN: Mfg. Engineering Technical Library
1	Department of the Army, Aerostructures Directorate, MS-266, U.S. Army Aviation R&T Activity - AVSCOM, Langley Research Center, Hampton, VA 23665-5225
1	NASA - Langley Research Center, Hampton, VA 23665-5225
1	U.S. Army Propulsion Directorate, NASA Lewis Research Center, 2100 Brookpark Road, Cleveland, OH 44135-3191
1	NASA - Lewis Research Center, 2100 Brookpark Road, Cleveland, OH 44135-3191
	Director, U.S. Army Materials Technology Laboratory, Watertown, MA 02172-0001
2	ATTN: SLCMT-TML
5	Authors

U.S. Army Materials Technology Laboratory
Watertown, Massachusetts 02172-0001
STRUCTURAL TESTING EFFORTS FOR M-102
HOWITZER SUBLENGTH COMPOSITE CRADLE -
Paul V. Cavallaro, Donald W. Oplinger,
Kanu R. Gandhi, Gregg J. Piper, and
Robert Pasternak

Technical Report MTL TR 92-13, March 1992, 30 pp-
illus-tables, D/A Project: 1L162105.AH84

AD________________
UNCLASSIFIED
UNLIMITED DISTRIBUTION

Key Words

Howitzer (105 mm)
Composites
Fiber reinforced composites

In support of the U.S. Army's Lightening the Force effort, the U.S. Army Materials Technology Laboratory (MTL) is conducting prototype development of artillery system components. The use of advanced materials such as fiber reinforced composites provides the key to obtaining considerable weight reductions without compromising structural integrity. Composite materials offer significant strength-to-weight ratios as well as unique tailorability features to suit the needs of the design engineer. Currently, composite applications to the M-102, 105 mm Howitzer system are in progress. This report discusses the related testing activities used to evaluate the present composite cradle design.

U.S. Army Materials Technology Laboratory
Watertown, Massachusetts 02172-0001
STRUCTURAL TESTING EFFORTS FOR M-102
HOWITZER SUBLENGTH COMPOSITE CRADLE -
Paul V. Cavallaro, Donald W. Oplinger,
Kanu R. Gandhi, Gregg J. Piper, and
Robert Pasternak

Technical Report MTL TR 92-13, March 1992, 30 pp-
illus-tables, D/A Project: 1L162105.AH84

AD________________
UNCLASSIFIED
UNLIMITED DISTRIBUTION

Key Words

Howitzer (105 mm)
Composites
Fiber reinforced composites

In support of the U.S. Army's Lightening the Force effort, the U.S. Army Materials Technology Laboratory (MTL) is conducting prototype development of artillery system components. The use of advanced materials such as fiber reinforced composites provides the key to obtaining considerable weight reductions without compromising structural integrity. Composite materials offer significant strength-to-weight ratios as well as unique tailorability features to suit the needs of the design engineer. Currently, composite applications to the M-102, 105 mm Howitzer system are in progress. This report discusses the related testing activities used to evaluate the present composite cradle design.

U.S. Army Materials Technology Laboratory
Watertown, Massachusetts 02172-0001
STRUCTURAL TESTING EFFORTS FOR M-102
HOWITZER SUBLENGTH COMPOSITE CRADLE -
Paul V. Cavallaro, Donald W. Oplinger,
Kanu R. Gandhi, Gregg J. Piper, and
Robert Pasternak

Technical Report MTL TR 92-13, March 1992, 30 pp-
illus-tables, D/A Project: 1L162105.AH84

AD________________
UNCLASSIFIED
UNLIMITED DISTRIBUTION

Key Words

Howitzer (105 mm)
Composites
Fiber reinforced composites

In support of the U.S. Army's Lightening the Force effort, the U.S. Army Materials Technology Laboratory (MTL) is conducting prototype development of artillery system components. The use of advanced materials such as fiber reinforced composites provides the key to obtaining considerable weight reductions without compromising structural integrity. Composite materials offer significant strength-to-weight ratios as well as unique tailorability features to suit the needs of the design engineer. Currently, composite applications to the M-102, 105 mm Howitzer system are in progress. This report discusses the related testing activities used to evaluate the present composite cradle design.

U.S. Army Materials Technology Laboratory
Watertown, Massachusetts 02172-0001
STRUCTURAL TESTING EFFORTS FOR M-102
HOWITZER SUBLENGTH COMPOSITE CRADLE -
Paul V. Cavallaro, Donald W. Oplinger,
Kanu R. Gandhi, Gregg J. Piper, and
Robert Pasternak

Technical Report MTL TR 92-13, March 1992, 30 pp-
illus-tables, D/A Project: 1L162105.AH84

AD________________
UNCLASSIFIED
UNLIMITED DISTRIBUTION

Key Words

Howitzer (105 mm)
Composites
Fiber reinforced composites

In support of the U.S. Army's Lightening the Force effort, the U.S. Army Materials Technology Laboratory (MTL) is conducting prototype development of artillery system components. The use of advanced materials such as fiber reinforced composites provides the key to obtaining considerable weight reductions without compromising structural integrity. Composite materials offer significant strength-to-weight ratios as well as unique tailorability features to suit the needs of the design engineer. Currently, composite applications to the M-102, 105 mm Howitzer system are in progress. This report discusses the related testing activities used to evaluate the present composite cradle design.